

Electronic Supplementary Material (ESI) for Analyst.  
This journal is © The Royal Society of Chemistry 2019

**Electronic supplementary information**

**“Vanishing mass” in the Sauerbrey world: Quartz Crystal Microbalance study of self-assembled monolayers based on tripod-branched structure with tuneable molecular flexibility**

Sergii Kravchenko and Boris Snopok\*

V.Lashkaryov Institute of Semiconductor Physics, NAS Ukraine

41 Prospect Nauki , Kyiv, 03028, Ukraine.

E-mail: [snopok@isp.kiev.ua](mailto:snopok@isp.kiev.ua)

**Table of Contents**

**Table ST1**

Analysis of equivalent oscillator circuit characteristics for unmodified QCM PR and QCM PR modified by **S3HX** monolayer (+10562 Hz, positive shift).

**Table ST2**

Resonance frequency shifts after **S3HX** modification for 11 samples prepared under the same conditions.

**Table ST3**

Typical changes of RF of **S3HX** PR while being treated in a 3 mM CaCl<sub>2</sub> solution.

**Table ST4**

RF change under the formation of **S3HX** monolayer in the presence of Ca<sup>2+</sup>.

**Table ST5**

Values of saturation vapor pressure P (mmHg) at 20 °C and specific constants for calculation from the Antoine equation

**Table ST6**

Topographic characteristics of the surfaces of QCM electrodes based on silver films.

**Table ST7**

Adsorption of Benzene and Ethanol saturation vapors on **S3HX** monolayers.

**Figure S1**

FTIR absorption spectra for **S3HX** monolayer on the QCM PR surface.

**Measuring device**

A photograph of the frequency generation and measurement device.

**Table ST1.**

**Analysis of equivalent oscillator circuit characteristics for unmodified QCM PR and QCM PR modified by S3HX monolayer (+10562 Hz, positive shift).**

The surface coating induces the significant change of effective R, L and C values: the capacity C1 decreased by four times; the inductance L increased by five times; the resistance RR increased by twenty times. Q-factor (c.a. 43110) was drastically low relative to unloaded quartz resonator (c.a. 176570). So, both mass increasing (L) and mechanical energy dissipation process (Q) were detected.

Reference Fr: 30 000 000,00 Hz

Power: 1.00 mW Into 5.0 ohms

PL: No Load CL: 10.00 pF

Sample	FR	RR	C0	C1	L	Q	C0/C1	FL	FDIF	TS	I	PWR	RL
	KHz	Ohms	pF	fF	mH	k		KHz	Hz	ppm/pF	uA	uW	Ohms
10 KHz, without cover	30 039,07	20,38	3,82	1,47	19,06	176,57	2 592,86	30 040,67	1 600,56	3,86	6 939,57	981,36	38,91
10 KHz, S1 monolayer	30 112,09	344,54	2,17	0,36	78,51	43,11	6 097,35	30 112,53	440,20	1,20	834,87	240,15	510,25

**Description:**

The measured parameters

FR - series resonant frequency

RR - resistance at FR

C0 - static capacitance

C1 - motion capacitance

L - motion inductance

Q - quality factor

C0/C1 - ratio of C0 over C1

FL - load resonant frequency at a specific load capacitance

FDIF - difference in frequency between the calibrated frequency FR and the actual frequency (FL-FR)

TS - trim sensitivity of load measurement

I - current into crystal

PWR - power into crystal

RL - resistance at FL

The authors thank Dr. Lev Dayan for radio-physics measurements, data interpretation and fruitful discussion.

**Table ST2.**

**Resonance frequency shifts after S3HX modification for 11 samples prepared under the same conditions.**

Sample	Frequency shift ( $\Delta f$ , Hz) after	
	<b>S3HX</b> SAM formation	Immersion into DMF
1	-568	-
2	-856	+8066
3	+1364	+8567
4	+4060	-
5	+10501	-
6	+10862	-
7	+10974	-
8	+11083	+1128
9	+11481	-
10	+12265	+987
11	+12671	-

**Table ST3.**

**Typical changes of RF of S3HX PR while being treated in a 3 mM CaCl<sub>2</sub> solution.**

Sample	Frequency shift ( $\Delta f$ , Hz) after		
	<b>S3HX</b> SAM formation	Immersion in CaCl <sub>2</sub> solution	Heating at 55 °C
1	-341	-2555	+754
2	-864	-1739	+368
3	+1043	-265	-1133
4	+10929	-282	-2739

**Table ST4.**

**RF change under the formation of S3HX monolayer in the presence of Ca<sup>2+</sup>.**

Sample	Frequency shift ( $\Delta f$ , Hz) after	
	Formation of <b>Ca<sup>2+</sup>S3HX</b>	Immersion into DMF
1	+5120	+8612
2	+3693	+10138
3	+3097	+7909
4	+6774	+9886
5	+4186	+8006

## Table ST5

### Values of saturation vapor pressure P (mmHg) at 20 °C and specific constants for calculation from the Antoine equation

The main characteristic of saturated vapor above the liquid is saturated vapor pressure, which is calculated using the Antoine equation.

The Antoine equation is a vapor pressure equation and describes the relation between vapor pressure and temperature for pure components.

$$\ln P = A - \frac{B}{T + C}$$

where P is the vapor pressure (mmHg), T is temperature (°C) and A, B and C are component-specific constants.

Values of saturation vapor pressure for benzene and ethanol

Liquid	P (mmHg)	A	B	C
Benzol	74,7	15,9008	2788,51	-52,36
Ethanol	43,9	18,9119	3803,98	-41,68

## Reference.

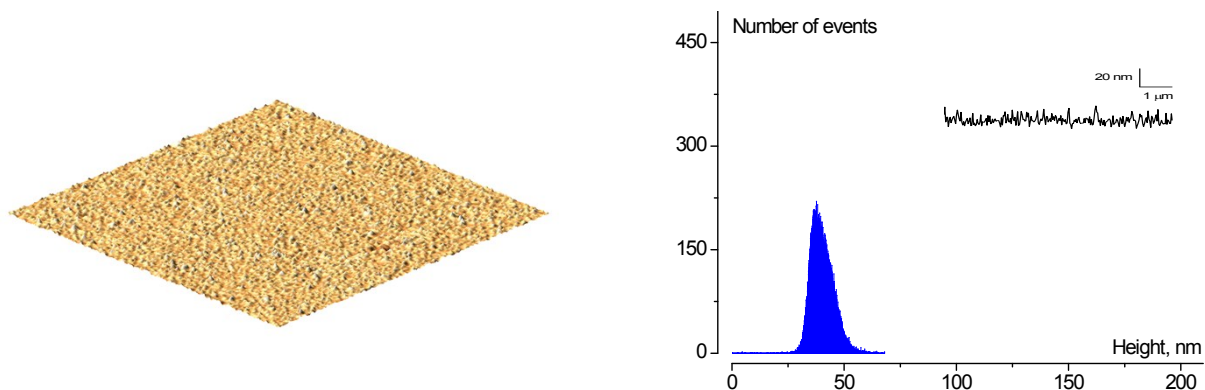
1. Antoine, C. // Tensions des vapeurs: nouvelle relation entre les tensions et les températures // Comptes Rendus des Séances de l'Académie des Sciences (in French)-V.107(1888), P.681–684.

2. Antoine, C. // Calcul des tensions de diverses vapeurs // Comptes Rendus des Séances de l'Académie des Sciences (in French)-V.107(1888), P.778–780.

## Table ST6

### Topographic characteristics of the surfaces of QCM electrodes based on silver films.

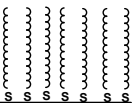
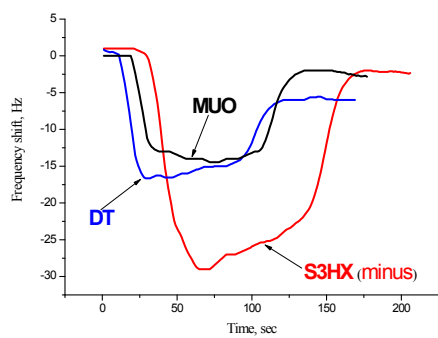
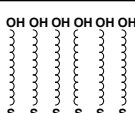
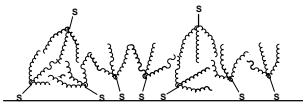
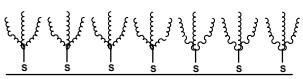
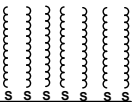
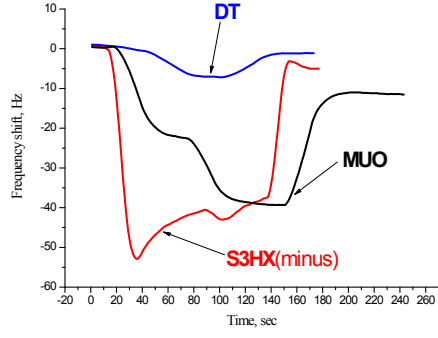
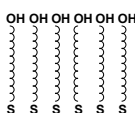
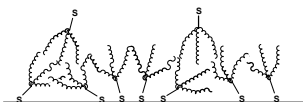
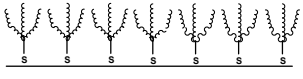
Topographic characteristics of the surfaces of QCM electrodes based on silver films. The surface images, as well as the calculation of the root mean square roughness (Roughness), are given for surface fragments of  $1 \times 1 \mu\text{m}$  in size.



Physical transducers of quartz microbalance are piezoelectric bulk wave resonators of the RK-169 type with resonant frequency of 10 MHz covered with silver electrodes 400 nm thick and 8 mm in diameter. Topographic analysis of the surface was carried out using an atomic force microscope (Nanoscope IIIa, Digital Instrument, Santa-Barbara) in tapping mode in air using probes based on silicon nitride.

Table ST7

Adsorption of Benzene and Ethanol saturation vapors on S3HX monolayers

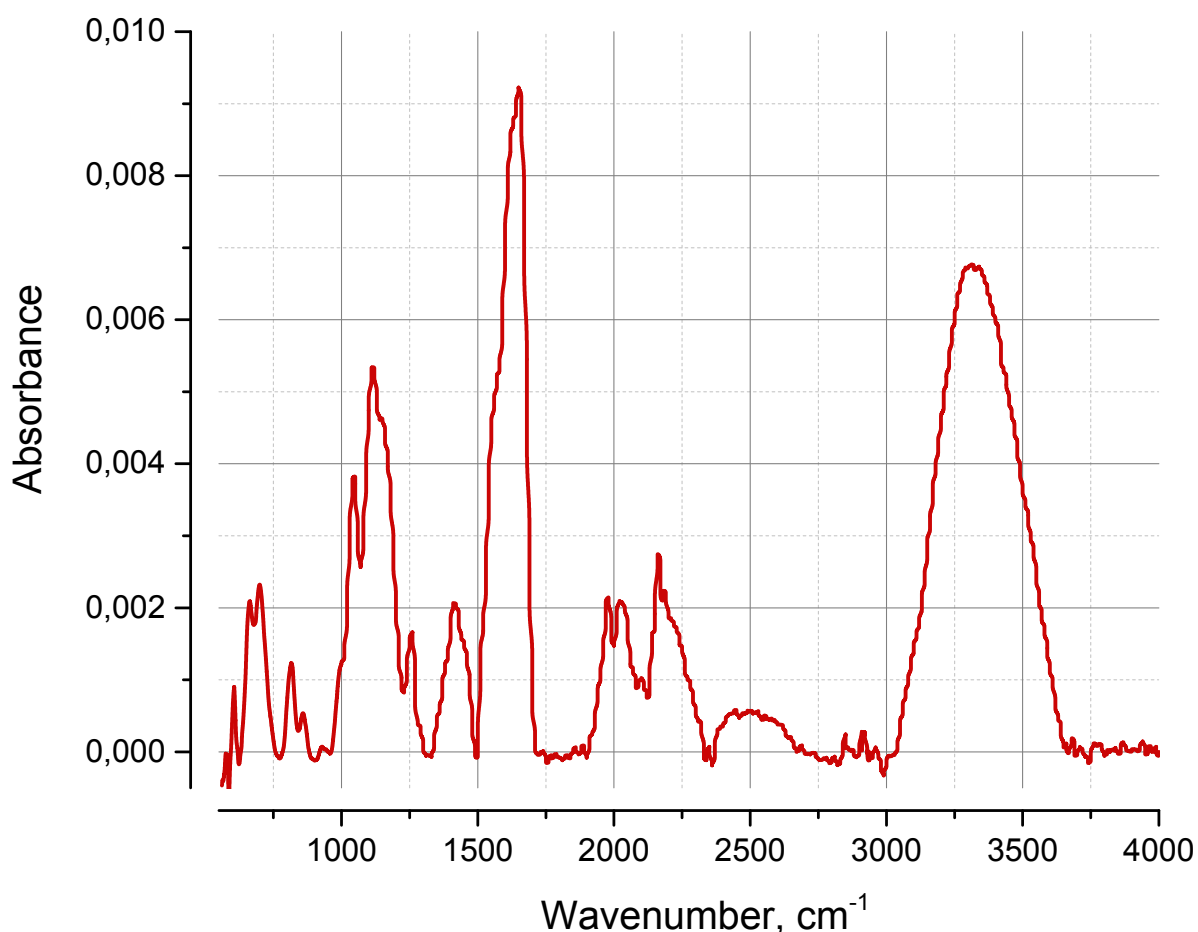
1	Benzol adsorption	DT		
		MUO		
		S3HX(minus)		
		S3HX(plus)		
2	Ethanol adsorption	DT		
		MUO		
		S3HX(minus)		
		S3HX(plus)		



**Figure S1**

**Absorption spectra of S3HX monolayer on the QCM PR surface**

The surface structures were characterized by infrared spectroscopy on a Nicolet 730 FTIR spectrometer with an ATR attachment.



The same compound was observed on the surface regardless of the sign of the RF shift after the surface layer formation. Presence of amide group was supported by both absorption bands near 1650 cm<sup>-1</sup> (C=O bond stretching vibration) and 1550 cm<sup>-1</sup> (N-H bond planar deformation vibration). Appearance of broad absorption band near 3300 cm<sup>-1</sup> indicated presence of bound hydroxyl-groups (O-H). UV reflection spectroscopy data <sup>27, 28</sup> as well confirmed that the same organic compound was present on the surface in the both cases.

**Figure S2**

**A photograph of the frequency generation and measurement device**



The frequency registration module, developed by Victor Volkov, Institute of Semiconductor Physics, is presented in Fig. S2. The corresponding high-level software was developed by Oleksii Snopok. The device includes a pre-counter and processor that provide frequency measurement, a flow switch, a reference frequency generator, and a RS-232 bus controller. The base of the device is a microcontroller. The program, recorded in the FLASH memory of the microcontroller, manages the status of the entire device as a whole, provides for the synchronization of commands and data via the RS-232 interface with the controlling computer, also controls the operation of the counter and switch.

The principle of operation of the system is based on the definition of the concept of frequency. That is, the system directly calculates the number of oscillations of the quartz plate that occurred within one second. In the frequency registration module, this is implemented as follows. After receiving a command from the control computer for frequency measurement, the microcontroller, whose speed is set by the reference generator, sends a reset signal to the pre-counter, setting it to zero. It then signals the account permission. The output values are increased by one with each new pulse of the quartz generators of the generator module. After passing a predetermined time interval (1 sec), counted on the reference generator, the microcontroller removes the signal "resolution of the account" from the input of the counter. The received data is sent to the control computer via the RS-232 interface. After receiving the data, the control computer can again request a frequency measurement.

The frequency measurement device is a stand-alone controller based on the AT89C2051 microprocessor, which is connected to a computer by a serial interface and is designed to measure the frequency of sensors based on piezo quartz resonators. The input signal is fed to the previous counter 74NS393, all outputs of which are connected to the microprocessor. The end result of the measurement is the total value of the previous counter (8 bits) and the internal microprocessor counter (17 bits), which at a time interval of one second allows you to record frequencies up to 32 MHz. The ADM232L chip matches the signal levels of the controller with the RS-232 standard, and the 7805 chip stabilizes the power supply. The frequency generation module is implemented on a specialized chip generator of Nippon Precision Circuits. The chip is designed to connect quartz resonators with a frequency of the fundamental harmonic from 3 to 40 MHz, while providing stable generation of rectangular pulses of a given amplitude. To eliminate the mutual influence of generators, to exclude the effect of "frequency capture" of adjacent channels for each generator, an inductive-capacitive filter in the power circuit is implemented.